ACADÉMIE
DES SCIENCES
INSTITUT DE FRANCE

Comptes Rendus
Chimie

Calogera Bertoloni, Vitalys Mba Ekomo, Benoît Villemejeanne, Charly Lemoine, Romain Duwald, Emmanuel Billy, Hakima Mendil-Jakani and Sophie Legeai

Propylene glycol-based deep eutectic solvent as an alternative to Ethaline for electrometallurgy

Volume 27, Special Issue S4 (2024), p. 203-214

Online since: 22 November 2024

Part of Special Issue: GDR Prométhée – French Research Network on *Hydrometallurgical Processes for Primary and Secondary Resources*

Guest editors: Laurent Cassayre (CNRS-Université de Toulouse, Laboratoire de Génie Chimique, France) and Hervé Muhr (CNRS-Université de Lorraine, Laboratoire Réactions et Génie des Procédés, France)

https://doi.org/10.5802/crchim.297

The Comptes Rendus. Chimie *are a member of the Mersenne Center for open scientific publishing*
www.centre-mersenne.org — e-ISSN : 1878-1543

ACADÉMIE DES SCIENCES
INSTITUT DE FRANCE

Comptes Rendus. Chimie
2024, Vol. 27, Special issue S4, p. 203-214
https://doi.org/10.5802/crchim.297

Research article

GDR Prométhée – French Research Network on *Hydrometallurgical Processes for Primary and Secondary Resources*

Propylene glycol-based deep eutectic solvent as an alternative to Ethaline for electrometallurgy

Calogera Bertoloni [a], Vitalys Mba Ekomo [b], Benoît Villemejeanne [c], Charly Lemoine [c], Romain Duwald [c], Emmanuel Billy [c], Hakima Mendil-Jakani [b] and Sophie Legeai [*, a]

[a] Institut Jean Lamour, Groupe Chimie et Electrochimie des Matériaux, UMR CNRS 7198—Université de Lorraine, 1 Boulevard Arago, BP 95823, 57078 Metz Cedex 3, France

[b] Laboratoire Systèmes Moléculaires et nanoMatériaux pour l'Énergie et la Santé (SyMMES), Commissariat à l'énergie atomique site de Grenoble, France

[c] Laboratoire des technologies de Valorisation des procédés et Matériaux pour les EnR (LVME), Commissariat à l'énergie atomique site de Grenoble, France

E-mail: sophie.legeai@univ-lorraine.fr (S. Legeai)

Abstract. Deep eutectic solvents (DESs) are of particular interest for electrometallurgy processes, since intrinsically conductive and electrochemically stable in a wide range of potentials. Cheaper and greener than conventional ionic liquids, DESs are often bio-sourced and exhibit a higher biodegradability. Ethaline, a DES composed of choline chloride (ChCl) as hydrogen bond acceptor and ethylene glycol (EG) as hydrogen bond donor in 1:2 molar proportions (Et 1:2), is commonly used in electrometallurgy thanks to its good transport properties. However, if ChCl can be considered as a "green" reactant, this is not the case for EG. A DES with a lower toxicity can be obtained by replacing EG by propylene glycol (PG), widely used in cosmetics and pharmacology, yielding a DES called Propeline. The present paper explores the potential of this lesser-known DES in the electrometallurgy of precious metals. Because changing the hydrogen bond donor leads to a modification in the DES bulk properties, the first part of this work deals with the determination of PG-based DESs' density, viscosity, and conductivity, which are properties of interest for electrochemical processes. The influence of water and PG content is presented and values are compared to those of Ethaline. It appears that ChCl:PG in a molar ratio 1:3 (Pr 1:3) presents the best transport properties. The potentiality of this solvent for the electrometallurgy of precious metals is then discussed: electrochemical stability and electrochemical systems of Ag, Pd, and Au are compared in Pr 1:3 and Et 1:2. Finally, diffusion coefficients of the metallic species and the DES components are given, determined by electrochemical and NMR techniques, respectively.

Keywords. Electrometallurgy, Deep eutectic solvent, Precious metals, Propeline, Transport properties.

Funding. Agence Nationale de la Recherche (EE4Precious project, ANR-20-CE08-0035-01).

Manuscript received 29 September 2023, revised 15 December 2023 and 30 January 2024, accepted 2 February 2024.

*Corresponding author

1. Introduction

The discovery of ionic liquids in 1914 by Paul Walden [1] with beneficial properties (vapor pressure, flammability, modulation, viscosity, density, refractive index, electrical conductivity, and thermal stability) led to applications such as electrochemistry, extraction, synthesis, analytical chemistry discussed by Kaur et al. [2]. These ionic liquids have also been used as additives in cosmetic products or as corrosion inhibitors [2,3]. An ongoing need to improve existing properties has led to the emergence of new so-called deep eutectic solvents (DES) based on the mixture of a proton acceptor (HBA) and a proton donor (HBD), first presented by Abbott et al. [4]. The first DES studied was a mixture of choline chloride as HBA and urea as HBD, and the resulting solvent was named Reline. Reline has properties similar to ionic liquids, which intended it for the same applications, but with a better control over the properties mentioned above and a reduced cost due to easier synthesis and composition modulation. As for ionic liquids, the conductivity of DESs and their complexing properties intend them for applications in electrochemical processes of metals. In the field of metal recycling, electrometallurgy in DES can be an alternative to toxic aqueous electrolytes (cyanides) for the recovery of precious metals for example, by consecutive electrochemical leaching and electrodeposition. The most popular DES for electrometallurgy applications is Ethaline which is based on the eutectic mixture of choline chloride (ChCl) and ethylene glycol (EG), i.e., in the 1:2 molar proportion [5–8]. Ethaline has more suitable properties for electrometallurgy (for example, low viscosity, better conductivity) than other DESs, even Reline. Most of the studies on DESs have thus been devoted to Ethaline. To date, a more ecological approach and a need to associate it with a reduction in costs guide research towards DESs that are more respectful of the environment and less expensive. Although the toxicity of eutectic mixtures is weakly investigated, databases are full of information on the toxicity of HBD. Several studies were published that call into question the harmlessness of some DESs considered as natural, thus showing that natural is not synonymous with green for environment [9]. The conclusion of such studies ultimately shows a certain unexpected toxicity of some DESs [10]. These studies also highlight the in-vivo toxicity of DESs compared to the individual elements (HBA and HBD) and the influence of their molar ratio [10,11]. In summary, studies have shown that DESs based on choline chloride as HBA have rather low toxicity [12,13] but that their toxicity increases with the toxicity of the HBD and thus with its molar ratio [10,11,14]. It is then reasonable to expect that the less toxic a HBD is, the less toxic the resulting DES will be.

In this work, to look for a DES with a lower toxic profile than Ethaline, ethylene glycol was switched by propylene glycol as HBD. The choice fell on propylene glycol because it shows the advantage of being a lot less toxic than ethylene glycol, known to be lethal for humans as well as terrestrial and aquatic animals by drinking water contamination. The structure of propylene glycol derives from ethylene glycol based on substitution of a proton by a methyl functional group. In addition, the use of propylene glycol instead of ethylene glycol is still economically viable, as the price of both solvents is similar (78 €/L, December 2023)[1] to propylene glycol price (50 €/L, December 2023)[2] according to Sigma Aldrich for a same *reagent grade* (>99%). Aware that the change of HBD leads to a modification of DES properties, and that these properties condition the applications of DESs, the first part of this work will deal with the investigation of relevant transport properties such as density, viscosity, and conductivity depending on the HBD choice, either ethylene glycol or propylene glycol. In addition, the possibility of using the prepared PG-based DESs for electrometallurgy applications will be presented by comparing their electrochemical properties to those of Ethaline and studying the electrochemical behavior of precious metals (Pd, Au, Ag) in these two DESs.

2. Experimental section

2.1. *Chemicals and materials*

The choline chloride (ChCl, 98%), ethylene glycol (EG, 99%), propylene glycol (PG, 99%) used for DES preparation, as well as ferrocene ($Fe[C_5H_5]_2{\cdot}6H_2O$,

[1] https://www.sigmaaldrich.com/FR/fr/product/sigald/102466.

[2] https://www.sigmaaldrich.com/FR/fr/substance/760957556.

98%), gold chloride ($AuCl_3$, >99.99%) and silver chloride (AgCl, >99%) were purchased from Sigma-Aldrich, France. Ethanol (EtOH, 96%) and palladium chloride ($PdCl_2$, 59%) were purchased from Merck France. Gold wire (99.99%), silver wire (99.99%) and palladium wire (99.95%) were purchased at Métalor Technologies France.

2.2. *DES preparation*

ChCl:EG (Et) and ChCl:PG (Pr) DESs were prepared respectively by mixing ChCl with EG, and ChCl with PG at 60 °C in a closed container under stirring. DESs were prepared at different molar ratios written down: HBA:HBD. When the influence of water content is studied, a third molar ratio is added in the name of the sample: HBA:HBD:H_2O. This ratio is expressed relative to HBA set at 1.

2.3. *Physico-chemical properties measurements*

All experiments were performed without any atmosphere control. The water content was measured by Karl Fischer coulometric titration using a Metrohm Karl Fischer 899 Coulometer with a HYDRANAL Coulomat E solution. Density was measured in a temperature range from 25 to 65 °C with 5 °C intervals, using an Anton Paar DMA 4100 M density meter, with a measurement accuracy of 10^{-4} g·cm^{-3}. Viscosity was determined using an Anton Paar AMVn viscometer with a repeatability of 0.1%. Conductivity was evaluated by potentiostatic electrochemical impedance spectroscopy (PEIS) using a Biologic Lab Potentiostat VSP 300. The conductivity cell was constituted of two parallel platinum plates, and the cell constant was determined using calibration samples (1.413; 5.0 and 12.8 mS·cm^{-1} at 25 °C). The sine wave amplitude was 10 mV, the studied frequency range extends from 1 MHz to 100 mHz with 6 measuring points per decade. The viscosity and the conductivity were measured in a temperature range of 25–60 °C with a step of 5 °C.

2.4. *Electrochemical characterizations*

All experiments were performed at 40 °C without any atmosphere control, using a Biologic Lab Potentiostat VSP 300. Au, Pd, and Ag were dissolved by anodic leaching of metallic wires, applying 1 mA·cm^{-2} in galvanostatic mode at 313 K in Et 1:2 and 333 K in Pr 1:3. The coulombic charge was adapted to the targeted concentration. Final concentrations were determined by the weight loss of the anode. Counter electrode (CE) was separated from the bulk electrolyte by a fritted glass to avoid electrodeposition of leached metals on the CE. Resulting electrochemical systems were studied by cyclic voltammetry. Electrochemical stability and electrochemical systems of metallic species were studied by cyclic voltammetry (CV) at a scan rate of 20 mV·s^{-1}. For CV experiments, the working electrode (WE) was a Pt disk of 2 mm in diameter. The CE and the reference electrode (RE) used in all electrochemical experiments were respectively a glassy carbon rod and an Ag^I/Ag electrode (Ag wire immersed in the studied DES containing 10 mM AgCl). The RE was calibrated against Fc^+/Fc (E^0 (Fc^+/Fc) = 0.63 V/SHE). All potential values measured in this study are therefore relative to SHE (standard hydrogen electrode).

2.5. *NMR measurements*

All NMR spectra were recorded with a Bruker Neo 400 MHz NMR spectrometer, equipped with a BBFO smartprobe. DOSY experiments were performed with Bipolar Pulsed Pair Stimulated Echo (BPSTE) pulse sequence. Each DOSY-NMR was based on 16 BPSTE-recorded spectra with 8 K data points. The diffusion time was 750 ms. The duration of the pulse field gradient was adjusted in a 600–2000 ms range in order to obtain 2–5% residual signal with the maximum gradient strength. The gradient strength was incremented in 16 steps from 5 to 95% of its maximum value in a linear ramp. Data processing was performed using Topspin 4.0.9 software.

3. Results and discussion

3.1. *Density*

Density (ρ) and its temperature dependence are important physical properties, which are useful for designing industrial processes. Densities of ChCl:EG and ChCl:PG DESs with HBA:HBD molar ratio 1:2 and 1:3 were measured in a 293–333 K temperature range at low and similar water content. The results are reported in Figure 1. The density of both DESs decreases with increasing temperature. This phenomenon is due to thermal expansion associated

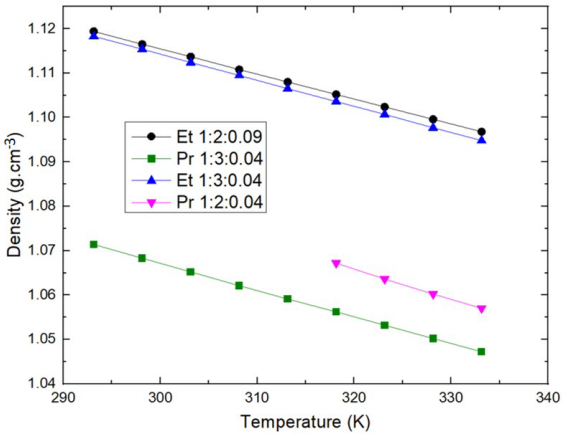

Figure 1. Density comparison of ChCl:EG and ChCl:PG DESs at different HBA:HBD ratios as a function of temperature.

with hydrogen bonding, and follows a linear temperature dependence.

Values were not measured under 318 K for Pr 1:2 (Propeline) because it is solid at lower temperatures. Moreover, there is a decrease in DES density with increasing HBD molar ratios, with much more impact on ChCl:EG than on ChCl:PG DESs given the difference observed. In the cases where only density matters, this would mean that the properties of ChCl:PG DESs would be more easily modulated than the properties of ChCl:EG DESs. The density of ChCl:PG DESs is lower than the density of ChCl:EG DESs whatever the HBA:HBD ratio. The values measured in this study are in accordance with existing literature [15,16]. Knowing that the density of ethylene glycol is higher than that of propylene glycol, it can be concluded that the density of the resulting DES is directly related to the density of the HBD. Wang et al. had already made the same observation by comparing the density of a larger number of DESs and concluded that the molar mass as well as the density of the HBD had a very large impact on the density of the resulting DES [17]. The density partially reflects the interaction strength between HBA and HBD components, which is ascribed to the strong hydrogen bond ability. This notable difference of density might be attributed to a different molecular organization or packing of the DES, changing the size of the HBA/HBD association spheres and leading to more free volume in ChCl:PG than in ChCl:EG DESs [18]. The extra methyl group of propylene glycol could be responsible for this by steric hindrance.

3.2. *Viscosity*

Viscosity is a very important information to relate the macroscopic properties linked to matter transport and hydrodynamic flow to the microscopic phenomena from which these macroscopic properties most often find their explanation.

The impact of temperature (Figure 2a) on ChCl:EG and ChCl:PG DESs' viscosity has been measured for 1:2 and 1:3 ratio. Increasing the HBD fraction clearly makes viscosity decrease for both DESs. Besides, viscosity of Pr 1:3 is higher than that of Et 1:3. This seems logical as propylene glycol alone is more viscous than ethylene glycol (56 and 21 mPa·s at 293 K, respectively). Several studies in the literature have already corroborated this observation: the decrease can be related to the formation or strengthening of hydrogen bonds, resulting in loss of molecular mobility as it closes free volume, on which the viscosity depends [15,16,19]. As for all liquids, the viscosity of ChCl:EG and ChCl:PG DESs decreases when temperature increases, due to thermal dilatation. The higher viscosity of ChCl:PG DESs suggests that they would be less interesting than ChCl:EG DESs, however it has to be noticed that both viscosities tend to get closer as temperature increases. Giving the fact that Pr 1:2 (Propeline) is solid under 318 K, and that it is very viscous compared to Et 1:2 (Ethaline) and Pr 1:3, further characterizations reported in this work will only concern Pr 1:3 in comparison to Et 1:2.

The influence of water content was studied by adding variable amounts of water from 600 to 47,000 ppm, which corresponds to ChCl:PG:H_2O molar ratios from 1:3:0.01 to 1:3:0.818. Viscosity measurements of Et 1:2 at similar water contents were added for comparison purpose (Figure 2b).

The increase in water content leads to a decrease in viscosity of both Et 1:2 and Pr 1:3. Water content therefore seems to be another interesting way to modulate the transport properties of Pr 1:3 [20]. Tuning temperature and water content of Pr 1:3 could then allow this DES to remain in the range of viscosity considered for ionometallurgical recycling applications, however keeping in mind that a high water content could destabilize the chloro-metallic

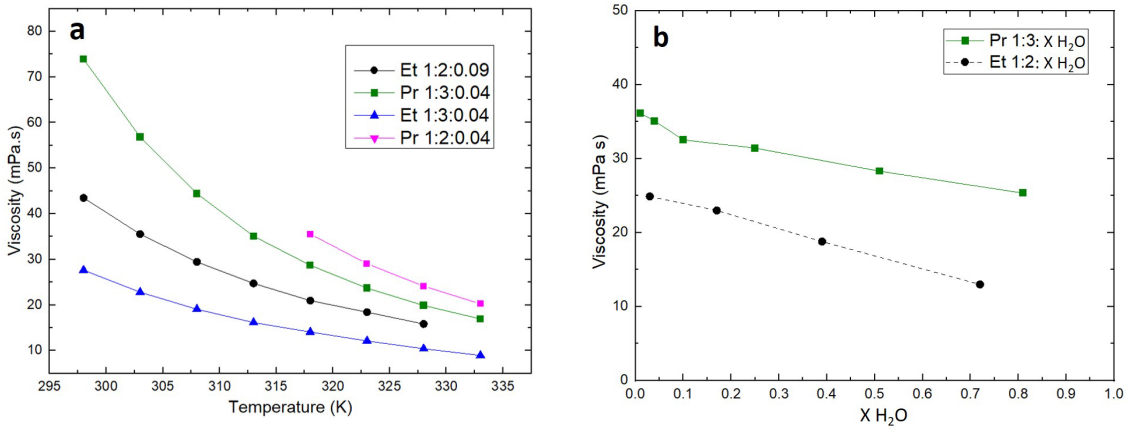

Figure 2. Viscosity of the DESs depending on (a) temperature and (b) water content at 313 K.

complexes or even lead to the formation of insoluble metallic species.

3.3. *Conductivity*

Figures 3a and 3b show the conductivity values of Et 1:2 and Pr 1:3 normalized by the ChCl molar ratio, as a function of temperature and water content, respectively. Ch^+ and Cl^- being the conductive species of the DESs, this representation allows to free oneself from the difference in ChCl proportion between the two considered DESs.

The conductivity of both DESs increases with temperature (Figure 3a). This is linked to the decrease in viscosity allowing faster ion diffusion. Indeed, the Walden plot ($\log(\Lambda)$ vs $\log(1/\eta)$) based on the Walden equation ($\Lambda \cdot \eta^{\alpha} = C$, Λ being the molar conductivity, η the viscosity and α and C constant parameters) presented in SI as Figure SI1 clearly shows that a linear fit can be obtained, meaning that only the viscosity impacts the molar conductivity.

The high viscosity of Pr 1:3 compared to Et 1:2 reflects a slower flow rate related to van der Waals and hydrogen interactions in the network, more important in Pr 1:3 than in Et 1:2. As well as the higher viscosity, hydrogen interactions in Pr 1:3 also help to explain the observed lower conductivity compared to Ethaline. Besides, Abbott et al. [21,22] put forward the theory of holes, which explains the viscosity of DESs. In DESs, not only molecular interactions tend to oppose the transport of ionic species, but also the holes generated by these interactions which leave inter- or intramolecular spaces. The size of these holes depends on hydrogen bond strength, temperature, and water content. Smaller holes will increase the viscosity, while larger holes will decrease it, and so hinder or enhance ion mobility, respectively.

Figure 3b shows that the conductivity of Ethaline remains higher than that of Pr 1:3 regardless of the water content. The review article published by Bryant et al. [23] on the interfacial nanostructure and the properties of ChCl:glycerol DES shows that water can be considered as a co-HBD for molar content higher than 5%, as a structural modification of DES was observed above this value. Below 25%, only the alignment of the liquid structure was modified. Alfurayj et al. [20] demonstrated that modest amounts of water addition (1–10%) to Ethaline are of little concern for practical use and can even lead to performance improvements, such as accelerated solvation and higher conductivity.

Knowing this behavior, Pr 1:3 therefore remains an interesting electrolyte as an alternative to Et 1:2 with reduced cost and environmental impact. Its similar physico-chemical properties can be easily modulated by temperature and water addition.

3.4. *Electrochemical stability*

Electrochemical stability, commonly called electrochemical window (EW), is one of the parameters of interest sought in DESs and ionic liquids, because they often show at least similar or even higher stability compared to common aqueous electrolytes [24–27]. For electrometallurgy applications, this characteristic is of primary importance, especially to avoid

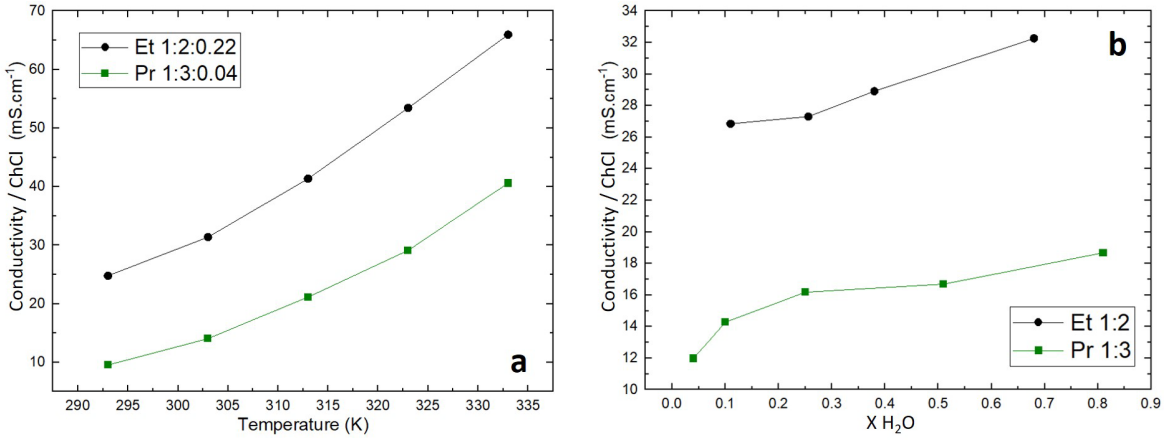

Figure 3. Conductivity of the DESs depending on (a) temperature and (b) water molar ratio at 298 K.

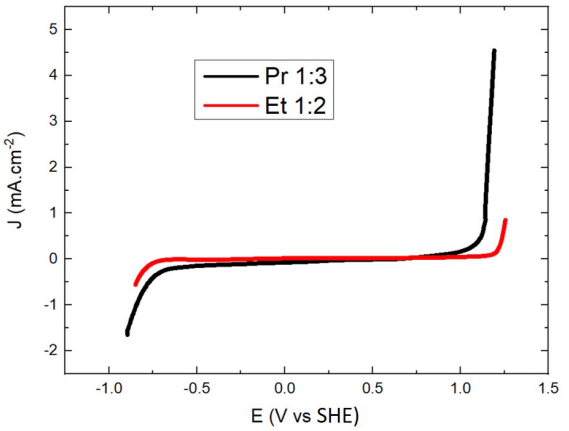

Figure 4. Electrochemical window of Et 1:2 and Pr 1:3 recorded by linear sweep voltammetry on a Pt working electrode at 20 mV·s^{-1} and 313 K.

DES degradation, which is more critical than water electrolysis using aqueous electrolytes, for cost and environmental reasons. The EW of Pr 1:3 was determined at a temperature of 313 K and compared to the EW of Et 1:2, widely used by the Abbott et al. group for electrometallurgy applications [28,29]. Figure 4 shows that the EW of Pr 1:3 ranges from −0.8 to 1.1 V vs SHE, very similar to the one of Et 1:2, as already observed by Costa et al. in the case of Pr 1:2 [30]. The oxidation signal recorded above 1.1 V vs SHE is usually attributed to EG/PG or chloride oxidation, whereas the reduction signal around −0.8 V vs SHE is associated to cholinium cation reduction [31].

The low difference in stability between the two DESs suggests that Pr 1:3 could replace Ethaline in electrometallurgical recycling processes. In addition, the potential ranges determined are comparable to those defined in the literature and frame the redox potentials of numerous electroactive metals of interest (gold, silver, palladium, etc.) [8,32]. The electrochemical stability of DESs can be somewhat limited by the amount of water. Valverde et al. [33] showed that the electrochemical window of Ethaline can vary by around 0.2 V with varying water amount from 1 to 15%.

3.5. *Electrochemical characterizations of precious metals*

In electrometallurgy, the oxidation and reduction potentials of metallic species are an indicator of their ability to be reduced (i.e., electrodeposited) or oxidized (i.e., electrochemically leached) in a specific electrolyte. Corresponding potential values must be included in the EW of the electrolyte. For that, Au, Pd, and Ag were dissolved by anodic leaching of metallic wires in Et 1:2 and Pr 1:3, and resulting electrochemical systems were studied by cyclic voltammetry. The superposition of the voltammograms in Figures 5a (Pr 1:3) and 5b (Et 1:2) allowed to compare the redox potentials of the chloro-metallic complexes formed in the two DESs, but also to define the possibility to leach, deposit, and so electrochemically recycle corresponding metals in both DESs.

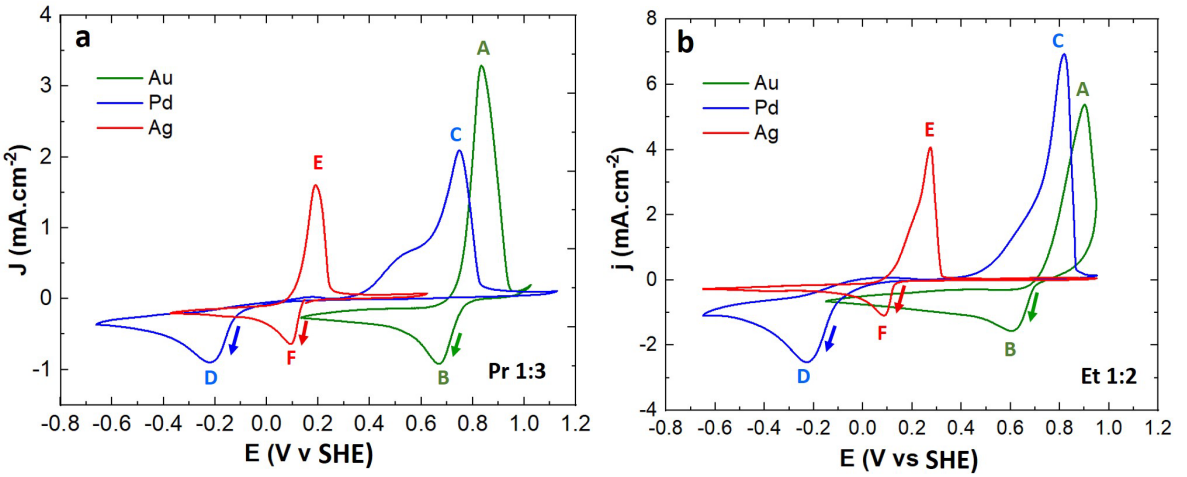

Figure 5. Cyclic voltammograms of Au(I), Pd(II) and Ag(I) monometallic leachates in (a) Pr 1:3 ([Au(I)] = 50 mM, [Ag(I)] = 16 mM, [Pd(II)] = 50 mM) and (b) Et 1:2 (([Au(I)] = 25 mM, [Ag(I)] = 25 mM, [Pd(II)] = 25 mM) recorded on Pt at 313 K at a scan rate of 20 mV·s^{-1}.

Obviously, Pd(II)/)Pd(0) is a non-reversible system with a slow charge transfer kinetics, as reduction and oxidation signals are separated by almost 0.9 V. As can be observed on the figures SI2 and SI3, the peak potential of Ag(I) and Au(I) reduction varies with the scan rate, meaning that these systems are not fully reversible. Here the redox system attribution is based on our previous work (Villemejeanne 2022) and literature data [34,35] in Et 1:2.

Table 1 and Figure 6 summarize the formal redox potential E_{app} (V vs SHE) determined from cyclic voltammograms according to Abbott et al. [36,37] using the average of onset potentials of the oxidation and reduction waves for each redox couple. The values obtained are compared to those published by Abbott et al. in 2011 using Et 1:2 [36,37].

It appears that all the redox potentials are included in the EW of Pr 1:3 determined in 3.4. The formal redox potential values are offset by approximatively 150–210 mV compared to Abbott et al. values, despite Abbott values being corrected to SHE reference electrode. Nevertheless, the oxidation and reduction peaks of metals determined in this work, are very close for Et 1:2 and Pr 1:3. The difference for a same metal does not exceed 100 mV. The distinct potentials for the reduction or oxidation of considered metallic species show a possibility for some to be leached and/or recovered. Depending on the targeted application, values extracted from the voltammograms are useful to determine the range of potential to apply. Indeed, to leach a metal, the applied potential has to be on the ascending part of the oxidation peak or superior to it, while for electrodeposition, the applied potential has to be on the descending part of the reduction peak or inferior to it. However, in case of a mix of metallic species, it would be possible to leach or deposit some but not

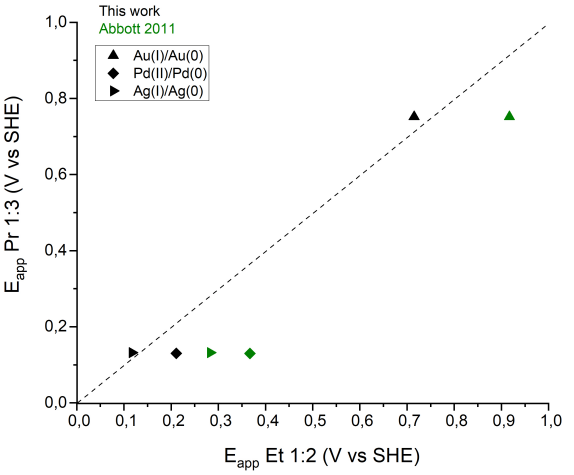

Figure 6. E_{app} of Au(I)/Au(0), Pd(II)/Pd(0) and Ag(I)/Ag(0) in Pr 1:3 vs E_{app} of Au(I)/Au(0), Pd(II)/Pd(0) and Ag(I)/Ag(0) in Et 1:2. Black labels: this work, green labels: Et1:2 values extracted from Abbott et al.

Table 1. Formal redox potentials of Au(I)/Au(0), Pd(II)/Pd(0) and Ag(I)/Ag(0) in Et 1:2 and Pr 1:3

Peaks	Redox couple	E_{app} (V vs SHE) *In italics: Abbott 2011*	
		Pr 1:3	Et 1:2
A/B	Au(I)/Au(0)	0.752	0.715
			0.917
C/D	Pd(II)/Pd(0)	0.130	0.211
			0.367
E/F	Ag(I)/Ag(0)	0.132	0.117
			0.283

all. Considering increasing oxidation potentials, Ag would be leached first, then Pd, and finally Au. In opposition, considering decreasing reduction potentials, the deposition would happen first with Au, then Ag, and finally Pd. It would not be possible to leach and recover Pd alone for example.

The CVs presented above also allow to calculate the diffusion coefficient of each metallic species leached in the DESs. The diffusion coefficient is a key parameter in electrometallurgy, contributing to the process efficiency. The deposition diffusion coefficients were calculated using the Berzins–Delahay Equation (Equation (1)) which takes into account the changes at the surface of the working electrode due to the metal deposition process.

$$I_{BD} = 0.6105AC(nF)^{3/2}\sqrt{Dv/RT}. \quad (1)$$

I_{BD} is the current intensity of the cathodic peak, A is the electrode area, C the concentration of the metallic ion, n the number of electrons transferred in the reduction reaction, F the Faraday constant, D the diffusion coefficient of the metallic ion, v the scan rate, R the gas constant and T the temperature. In order to verify that the diffusion of species is the driving force at this scan rate value, scan rate v was varied between 5 and 100 mV/s in the case of the Ag electrochemical system. Figure SI4 shows that the Ag(I) reduction peak current i_{peak} is proportional to $v^{1/2}$ in the whole scan rate range tested for Pr 1:3 and Et 1:2. The diffusion laws can then be applied to calculate the diffusion coefficient from CV runs at 20 mV/s for all metallic species. The diffusion coefficients calculated at 313 K, for a concentration of 50 mM of salts in Pr 1:3 and 25 mM in Et 1:2, are displayed in Table 2.

Table 2. Diffusion coefficients of metallic species in Et 1:2 and Pr 1:3

	Ag(I)	Pd(II)	Au(I)
$D_{Pr\,1:3}$ ($m^2{\cdot}s^{-1}$)	2.5×10^{-11}	6.3×10^{-12}	5.2×10^{-11}
$D_{Et\,1:2}$ ($m^2{\cdot}s^{-1}$)	1.9×10^{-10}	1.2×10^{-11}	3.9×10^{-11}

The diffusion coefficients of the considered metallic species in Pr 1:3 are almost the same or at mostone order of magnitude lower than in Ethaline. Au(I) shows the fastest diffusion and Pd(II) the lowest for both DESs. These values are comparable to those previously published in Et 1:2 (Ag [38,39], Au [39,40], Pd [36,37,41]) and are higher than those determined in Reline [41–43], a DES often used in electrometallurgy.

3.6. *NMR characterization of Pr 1:3/metal salts solutions*

3.6.1. *Identification of DES solution structure*

The solution structure of Pr 1:3 was investigated by ^{1}H NMR, and compared to the solution structure of Et 1:2 as a reference. DESs were characterized as pure solvents, without the use of a deuterated diluent. Regarding the Pr 1:3 spectrum, the ^{1}H NMR signals corresponding to ChCl are observed at 5.02, 3.68, 3.31, and 2.98 ppm. The signals corresponding to PG are seen at 4.57, 3.45, 3.09, and 0.78 ppm (Figure 7, top). The NMR spectra of Et 1:2 exhibit signals at 5.24, 3.99, 3.61, and 3.30 ppm for ChCl, and 4.78 and 3.58 ppm for EG. In both DESs, the most unshielded signals correspond to labile protons *a* of ChCl and *e* and *h* protons of PG or *f* protons of EG for Pr 1:3 or Et 1:2, respectively.

The influence of metallic species was studied by addition of metallic salts (AgCl, $PdCl_2$, $AuCl_3$). Interestingly, upon addition of previously listed metals in Pr 1:3 (Figure 8), it appears that interactions between DESs and metallic species are not systematically the same. In fact, no differences can be seen between Pr 1:3 with and without $PdCl_2$ or AgCl. Nevertheless, in presence of $AuCl_3$, it appears that all labile protons from OH groups are fused (Figure 8, green). The fusion of those signals is explained by a fast exchange of the protons from the hydroxyl groups.

As well as for Pr 1:3, there is no observable effect of $PdCl_2$ in the solution structure of Et 1:2 in ^{1}H NMR

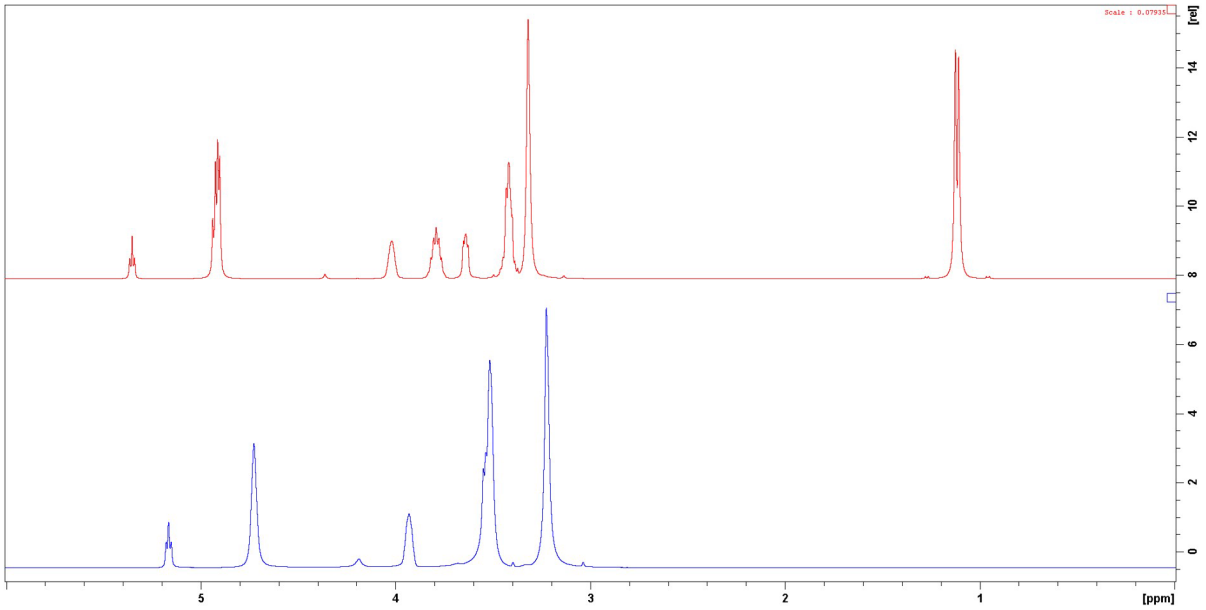

Figure 7. ^{1}H NMR spectra of Pr 1:3 (top) and Et 1:2 (bottom).

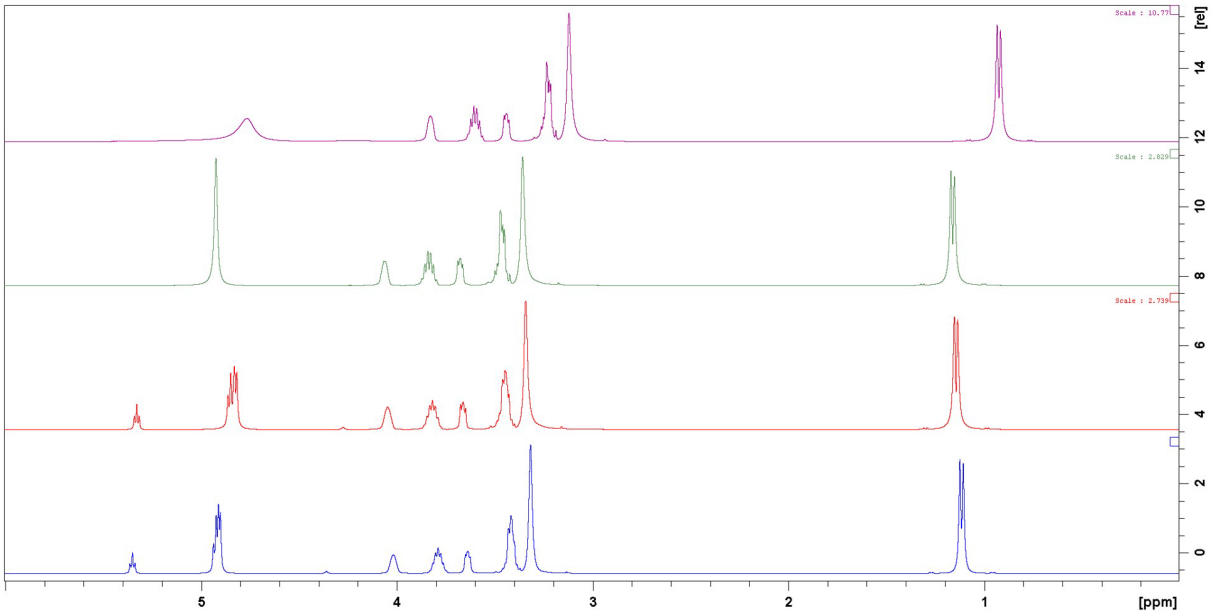

Figure 8. ^{1}H NMR spectra of Pr 1:3 (blue), and Pr1:3 + $PdCl_2$ (red), Pr 1:3 + $AuCl_3$ (green) and Pr 1:3 + AgCl (purple).

(Figure 9). Nevertheless, a broadening of OH signals corresponding to a fast exchange is observed in the presence of $AuCl_3$ and AgCl salts.

3.6.2. *PFG-NMR analyses*

Diffusion experiments carried by NMR allows an in-depth comprehension of solvent/metals interac-

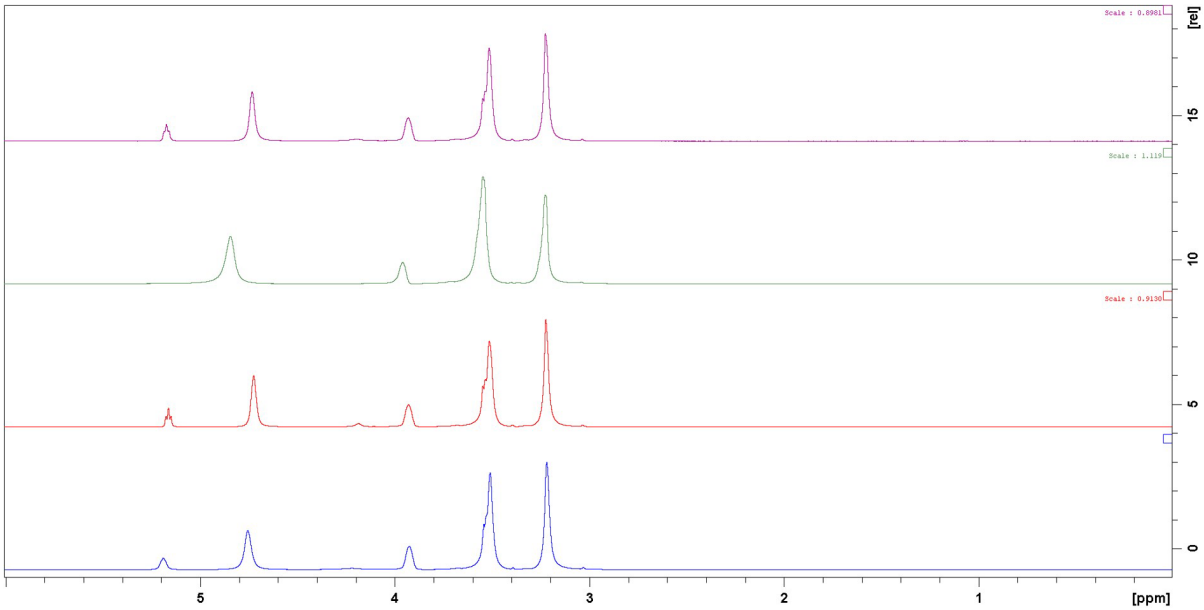

Figure 9. ^{1}H NMR spectra of Et 1:2 (blue), and Et 1:2 + $PdCl_2$ (red), Et 1:2 + $AuCl_3$ (green) and Et 1:2 + AgCl (purple).

tions. Diffusion-ordered spectroscopy (DOSY) with a decreasing magnetic field gradient from 95 to 5% were run at 313 K. The diffusion coefficient D of each species in solution is determined according to Debye–Einstein Equation (2), where the molecule is approximated as a spherical particle of hydrodynamic radius r_H, η is the viscosity of the solvent (mPa·s), k_B the Boltzmann constant, and T the temperature (K).

$$D = \frac{k_B T}{6\pi\eta r_H}. \quad (2)$$

The diffusion coefficients for choline chloride HBA and ethylene glycol or propylene glycol HBD are listed in Tables 3 and 4 for Et 1:2 and Pr 1:3, respectively. The diffusivity of aliphatic (D_{Ch+}) and hydroxyl ($D_{OH–Ch+}$) protons in the choline chloride moiety of Et 1:2 are slightly different (Table 3, entry 1). This is due to a fast exchange between hydroxyl protons of ChCl and water. Furthermore, the diffusivity of choline cations is lower than the diffusivity of HBD. This is due to the higher molecular weight and molecular size of the cation compared to those of the corresponding HDB. The diffusivity of aliphatic protons of ChCl (D_{Ch+}) and ethylene glycol (D_{EG}) in Et 1:2 are slightly decreased after dissolution of Pd(II), Au(III) or Ag(I) metal ions (Table 3, entries 2–4). Despite the increase in water fraction in the DES after metal salts dilution, which must be responsible for an increase in diffusivity, the decreasing diffusivity of both HBA and HBD species tends to indicate a strong interaction between the metal ions and the DES. These observations are in agreement with the study of Abbott et al. [44]. The diffusivity difference between aliphatic (D_{EG}) and acidic protons ($D_{OH–EG}$) of ethylene glycol indicates that the acidic protons are in fast exchange with some other species. This observation is reinforced by the disappearance of the OH–Ch^+ protons in the case of Au and Ag salts (Table 3, entry 3–4). The high water content of these solutions explains the rapid exchange between the labile protons of all the components of the solutions.

On the contrary, the metal salts dissolution has no marked influence on the diffusion coefficients of Ch^+ cation (D_{Ch+}) and propylene glycol (D_{PG}, $D_{OH–PG}$) in Pr 1:3 (Table 4). Two possibilities have to be considered (i) the third equivalent of HBD in the DES composition interacts preferentially with the metal ions rather than with the HBA/HBD association and (ii) the metal salts are not dissociated in Pr 1:3 and keep a neutral form instead of an ionic form. Indeed, as it was observed in the case of Et 1:2, the

Table 3. Diffusion coefficients for Et 1:2 solutions

	Ethaline	Composition HBA/HBD/H_2O	10^{-11} D_{Ch+} ($m^2{\cdot}s^{-1}$)	10^{-11} $D_{OH–Ch+}$ ($m^2{\cdot}s^{-1}$)	10^{-11} D_{EG} ($m^2{\cdot}s^{-1}$)	10^{-11} $D_{OH–EG}$ ($m^2{\cdot}s^{-1}$)
1	Et 1:2	1/2/0.09	4.18	7.69	7.55	7.92
2	Et 1:2 + Pd	1/2/0.18	3.17	5.65	5.39	6.78
3	Et 1:2 + Au	1/2/0.09	2.84	-	5.89	6.44
4	Et 1:2 + Ag	1/2/0.18	2.41	-	4.66	5.47

Table 4. Diffusion coefficients for Pr 1:3 solutions

	Pr 1:3	Composition HBA/HBD/H_2O	10^{-11} D_{Ch+} ($m^2{\cdot}s^{-1}$)	10^{-11} $D_{OH–Ch+}$ ($m^2{\cdot}s^{-1}$)	10^{-11} D_{PG} ($m^2{\cdot}s^{-1}$)	10^{-11} $D_{OH–PG}$ ($m^2{\cdot}s^{-1}$)
1	Pr 1:3	1/3/0.01	1.69	1.91	2.50	2.41
2	Pr 1:3 + Pd	1/3/0.01	1.72	2.17	2.55	2.65
3	Pr 1:3 + Au	1/3/0.09	3.32	-	5.17	5.06
4	Pr 1:3 + Ag	1/3/0.04	1.86	-	2.72	3.30

formation of a strong ionic pair between DES and metal ion lead to a decrease in diffusivity of both HBA and HBD species, even if the water ratio of the solution increases. The increase in diffusivity of HBA and HBD species in the case of Au dissolution is attributed to the increase in water content in the solvent (Table 4, entry 3).

4. Conclusions

From this work, it can be concluded that it is possible to consider Pr 1:3 as an alternative system to Ethaline for electroleaching/deposition applications, with the advantage of much lower toxicity. The electrochemical properties of Pr 1:3 and of precious metals studied here as examples, are similar to Ethaline. The slightly lower transport properties of ChCl-PG DESs could be circumvented by the modulation of HBD molar ratio and a moderate increase in working temperature or water content. Diffusion experiments carried by NMR showed that strong interactions exists between Ethaline and metallic species, whereas the dissolution of the same metals in Pr 1:3 had no influence on diffusion coefficients, indicating a different state of solvation in this solvent. The lower interaction between Pr 1:3 and metal ions should be a strength in the durability of the solvent during cycling. This will be a part of a future work.

Declaration of interests

The authors do not work for, advise, own shares in, or receive funds from any organization that could benefit from this article, and have declared no affiliations other than their research organizations.

Funding

This work has been supported by the Agence Nationale de la Recherche (EE4Precious project, ANR-20-CE08-0035-01).

Raw data

Raw data corresponding to this research work are available in open access at: https://doi.org/10.12763/EGL57A.

Supplementary data

Supporting information for this article is available on the journal's website under https://doi.org/10.5802/crchim.297 or from the author.

References

[1] P. Walden, *Bull. Acad. Imper. Sci.*, 1914, **8**, 405-422.
[2] G. Kaur, H. Kumar, M. Singla, *J. Mol. Liquids*, 2022, **351**, article no. 118556.

[3] M. Yadav, D. Behera, S. Kumar, R. R. Sinha, *Ind. Eng. Chem. Res.*, 2013, **52**, 6318-6328.
[4] A. P. Abbott, G. Capper, D. L. Davies, R. K. Rasheed, V. Tambyrajah, *Chem. Commun.*, 2003, **1**, 70-71.
[5] S. Ghosh, S. Roy, *Surf. Coat. Technol.*, 2014, **238**, 165-173.
[6] N. G. Sousa, C. P. Sousa, O. S. Campos, P. de Lima-Neto, A. N. Correia, *J. Mol. Liquids*, 2019, **288**, article no. 111091.
[7] N. Peeters, K. Janssens, D. de Vos, K. Binnemans, S. Riaño, *Green Chem.*, 2022, **24**, 6685-6695.
[8] A. P. Abbott, R. C. Harris, F. Holyoak, G. Frisch, J. Hartley, G. R. T. Jenkin, *Green Chem.*, 2015, **17**, 2172-2179.
[9] M. Hayyan, Y. P. Mbous, C. Y. Looi, W. F. Wong, A. Hayyan, Z. Salleh, O. Mohd-Ali, *SpringerPlus*, 2016, **5**, article no. 913.
[10] M. Hayyan, C. Y. Looi, A. Hayyan, W. F. Wong, M. A. Hashim, *PLoS One*, 2015, **10**, article no. e0117934.
[11] L. Lomba, M. P. Ribate, E. Sangüesa, J. Concha, M. P. Garralaga, D. Errazquin, C. B. García, B. Giner, *Appl. Sci.*, 2021, **11**, article no. 10061.
[12] K. Radošević, M. Cvjetko Bubalo, V. Gaurina Srček, D. Grgas, T. Landeka Dragičević, I. Radojčić Redovniković, *Ecotoxicol. Environ. Safety*, 2015, **112**, 46-53.
[13] K. Radošević, N. Ćurko, V. Gaurina Srček, M. Cvjetko Bubalo, M. Tomašević, K. Kovačević Ganić, I. Radojčić Redovniković, *LWT*, 2016, **73**, 45-51.
[14] R. Ahmadi, B. Hemmateenejad, A. Safavi, Z. Shojaeifard, M. Mohabbati, O. Firuzi, *Chemosphere*, 2018, **209**, 831-838.
[15] N. F. Gajardo-Parra, V. P. Cotroneo-Figueroa, P. Aravena, V. Vesovic, R. I. Canales, *J. Chem. Eng. Data*, 2020, **65**, 5581-5592.
[16] E. S. C. Ferreira, I. V. Voroshylova, N. M. Figueiredo, C. M. Pereira, M. N. D. S. Cordeiro, *J. Mol. Liquids*, 2020, **298**, article no. 111978.
[17] Y. Wang, W. Chen, Q. Zhao, G. Jin, Z. Xue, Y. Wang, T. Mu, *Phys. Chem. Chem. Phys.*, 2020, **22**, 25760-25768.
[18] Q. Zhang, K. De Oliveira Vigier, S. Royer, F. Jérôme, *Chem. Soc. Rev.*, 2012, **41**, 7108-7146.
[19] A. P. Abbott, S. Nandhra, S. Postlethwaite, E. L. Smith, K. S. Ryder, *Phys. Chem. Chem. Phys.*, 2007, **9**, 3735-3743.
[20] I. Alfurayj, C. C. Fraenza, Y. Zhang *et al.*, *J. Phys. Chem. B*, 2021, **125**, 8888-8901.
[21] A. P. Abbott, *ChemPhysChem*, 2004, **5**, 1242-1246.
[22] A. P. Abbott, G. Capper, D. L. Davies, R. Rasheed, *Inorg. Chem.*, 2004, **43**, 3447-3452.
[23] S. J. Bryant, A. J. Christofferson, T. L. Greaves, C. F. McConville, G. Bryant, A. Elbourne, *J. Colloid Interface Sci.*, 2022, **608**, 2430-2454.
[24] N. Sinclair, X. Shen, J. S. Wainright, *Meet. Abstr.*, 2021, **MA2021-01**, 25.
[25] M. H. Chakrabarti, F. S. Mjalli, I. M. AlNashef, M. A. Hashim, M. A. Hussain, L. Bahadori, C. T. J. Low, *Renew. Sustain. Energy Rev.*, 2014, **30**, 254-270.
[26] D. Lloyd, T. Vainikka, L. Murtomäki, K. Kontturi, E. Ahlberg, *Electrochim. Acta*, 2011, **56**, 4942-4948.
[27] R. Cheng, J. Xu, X. Wang, Q. Ma, H. Su, W. Yang, Q. Xu, *Front. Chem.*, 2020, **8**, article no. 619.
[28] A. P. Abbott, K. E. Ttaib, G. Frisch, K. J. McKenzie, K. S. Ryder, *Phys. Chem. Chem. Phys.*, 2009, **11**, 4269-4277.
[29] B. Villemejeanne, S. Legeai, E. Meux, S. Dourdain, H. Mendil-Jakani, E. Billy, *J. Environ. Chem. Eng.*, 2022, **10**, article no. 108004.
[30] R. Costa, M. Figueiredo, C. M. Pereira, F. Silva, *Electrochim. Acta*, 2010, **55**, 8916-8920.
[31] K. Haerens, E. Matthijs, K. Binnemans, B. Van der Bruggen, *Green Chem.*, 2009, **11**, 1357-1365.
[32] W. Sánchez-Ortiz, J. Aldana-González, T. Le Manh *et al.*, *J. Electrochem. Soc.*, 2021, **168**, article no. 016508.
[33] P. E. Valverde, T. A. Green, S. Roy, *J. Appl. Electrochem.*, 2020, **50**, 699-712.
[34] A. P. Abbott, G. Frisch, J. Hartley, W. O. Karim, K. S. Ryder, *Prog. Nat. Sci.: Mater. Int.*, 2015, **25**, 595-602.
[35] S. Datta, J. Mahin, E. Liberti, I. Manasi, K. J. Edler, L. Torrente-Murciano, *ACS Sustain. Chem. Eng.*, 2023, **11**, 10242-10251.
[36] C. D'Agostino, R. C. Harris, A. P. Abbott, L. F. Gladden, M. D. Mantle, *Phys. Chem. Chem. Phys.*, 2011, **13**, 21383-21391.
[37] A. P. Abbott, G. Frisch, S. J. Gurman, A. R. Hillman, J. Hartley, F. Holyoak, K. S. Ryder, *Chem. Commun.*, 2011, **47**, 10031-10033.
[38] F. Bohrn, M. Leitzenberger, S. Schwab, P. Kuegler, L. Brunnbauer, S. Jordan, H. Hutter, *ECS J. Solid State Sci. Technol.*, 2022, **11**, article no. 024006.
[39] S. Rahali, R. Zarrougui, M. Marzouki, O. Ghodbane, *J. Electroanal. Chem.*, 2020, **871**, article no. 114289.
[40] L. Aldous, D. S. Silvester, C. Villagrán, W. R. Pitner, R. G. Compton, M. Cristina Lagunas, C. Hardacre, *New J. Chem.*, 2006, **30**, 1576-1583.
[41] G. Lanzinger, R. Böck, R. Freudenberger, T. Mehner, I. Scharf, T. Lampke, *Trans. IMF*, 2013, **91**, 133-140.
[42] Y. Katayama, Y. Bando, T. Miura, *Trans. IMF*, 2008, **86**, 205-210.
[43] F. Soma, Q. Rayée, M. Bougouma, C. Baustert, C. Buess-Herman, T. Doneux, *Electrochim. Acta*, 2020, **345**, article no. 136165.
[44] A. P. Abbott, R. C. Harris, K. S. Ryder, *J. Phys. Chem. B*, 2007, **111**, 4910-4913.